TWO-MEASURED VARIABLE METHOD FOR WALL INTERFERENCE ASSESSMENT/CORRECTION

C. F. Lo and W. L. Sickles
Calspan Corporation/AEDC Division
Arnold Air Force Station, Tennessee

Summary

An iterative method for wall interference assessment and/or correction is presented specifically for transonic flow conditions in wind tunnels equipped with two-component velocity measurements on a single interface. The iterative method does not require modeling of the test article and tunnel wall boundary conditions. Analytical proof for the convergence and stability of the iterative method is shown in the subsonic flow regime. The numerical solutions are given for both two-dimensional and axisymmetrical cases at transonic speeds with the application of global Mach number correction.

Introduction

The recognition of the shortcomings of the classical methods for determining wall interference has demanded that a variety of flow measurements near or on the tunnel wall be made to assess wall interference. For example, Arnold Engineering Development Center has designed an interface measurement system for the 4-foot Transonic Tunnel and the wall pressure measurement system is being planned for installation in the current 12-ft Wind Tunnel restoration project at NASA/Ames Research Center. It is well known that classical methods require a mathematical modeling of the wall boundary condition which is a difficult task, in particular, for a ventilated wall. The characteristics of a ventilated wall are not precisely known and generally vary with Mach number, model geometry, Reynolds number and wall configuration. Another shortcoming is the necessity to accurately represent the test article beyond the simplified representation used in the classical approach.

Furthermore, the development of an adaptive wall tunnel requires that the boundary flow measurements be an integral part of the procedure. The boundary measurements are designed to determine adaptive-wall setting for free-air or noninterference condition. Techniques using only the measurements to assess the level of interference will complement the adaptive-wall process by determining if a noninterference wall setting has been achieved or by correcting for residual interference. Therefore, several wall interference methods based solely on the measured flow boundary condition have been developed for different kinds of measurements, such as two velocity components at a single interface (Refs. 1-4) or one velocity component at two interfaces (Ref. 5). However, all methods are limited to subsonic flow.

The purpose of this paper is to present a method for assessing wall interference for subsonic as well as transonic flow regimes based only on two velocity distributions measured on a single interface and no knowledge of the test article. This method as shown in Fig. 1 is divided into two tasks. The first task is the determination of the effective (equivalent) shape of the model from the two-measured variables by an iterative procedure. The second task is to predict the wall interference, such as a global Mach number correction, based on the effective shape predicted from Task 1.

In the presentation of the paper, a proposed iterative procedure to accomplish Task 1 is described and convergence analytically proved for subsonic flow. Numerical validation is demonstrated for two-dimensional and axisymmetrical transonic flows using a transonic small disturbance equation, and the global Mach number corrections are determined for Task 2.

Iterative Procedure of Effective Shape

To accomplish Task 1, an iterative procedure using two measured distributions of velocity near the wall has been developed and is shown in Fig. 2. The procedure consists of two basic steps in which each step involves obtaining a solution for the region between a measurement interface ($y=h$) and an effective shape line ($y=y_1$) near the model. In the first step, the velocity component, $u^o(y_1)$, is obtained from a solution of the region where the boundary conditions are provided by an initial guess of the effective shape $v^o(y_1)$, and the measured velocity component $u_t(h)$. With the result, $u^o(y_1)$, the second step obtains the solution $v^1(y_1)$ in the same region using the measured boundary condition $v_t(h)$. These two steps are repeated until convergence has been achieved and the effective shape, $v(y_1)$, determined.

Defining a merit function for the difference, $v^{n+1}(y_1) - v^n(y_1)$, one can relax the effective shape between iterations by the form of

$$v^{n+1}(y_1) = \omega\, v^{n+1}(y_1) + (1-\omega)\, v^n(y_1)$$

with ω as a relaxation factor. An updated effective shape, $v(y_1)$, is yielded by repeating Steps 1 and 2 with this relaxed form of velocity as input until the given criterion of merit function is satisfied.

Predicted Effective Shape

The iterative procedure for determining the effective shape is extremely flexible and can be applied to a variety of tunnel flow conditions. Depending on the flow condition, the region between the two surfaces could be analytically or numerically solved for the appropriate fluid equations, such as the Prandtl-Glauert equation, transonic small disturbance equation, full potential equation, or Euler equations. To illustrate the validity of the iterative procedure, it is applied to the two-dimensional, subsonic, Prandtl-Glauert equation. For this linear problem the solution for each iterative step can be determined analytically. The analytical expressions of the iterative solutions were derived by the Fourier transform technique as

$$u^n(x,y_1) = \frac{1}{2\beta(h-y_1)} \int_{-\infty}^{\infty} \frac{u_t(\xi,h)}{\cosh\left(\frac{\pi(\xi-x)}{2\beta(h-y_1)}\right)}$$

$$- \frac{1}{2\beta^2(h-y_1)} \oint_{-\infty}^{\infty} \frac{v^n(\xi,y_1)}{\sinh\left(\frac{\pi(\xi-x)}{2\beta(h-y_1)}\right)} d\xi \qquad (1)$$

$$v^{n+1}(x,y_1) = \frac{1}{2\beta(h-y_1)} \int_{-\infty}^{\infty} \frac{v_t(\xi,h)}{\cosh\left(\frac{\pi\xi-x)}{2\beta(h-y_1)}\right)} d\xi$$

$$+ \frac{1}{2(h-y_1)} \oint_{-\infty}^{\infty} \frac{u^n(\xi,y_1)}{\sinh\left(\frac{\pi(\xi-x)}{2\beta(h-y_1)}\right)} d\xi \qquad (2)$$

The convergence and stability of these iterative procedures has been proved analytically in Appendix A and Appendix B, respectively. The results for a NACA0012 airfoil at M = 0.6 in an open-jet tunnel are shown in Fig. 3. It can be seen that the predicted effective shape compares well with an independent reference calculation from the original airfoil profile.

For transonic flow, the numerical solution of the transonic small disturbance equation was solved for the procedure as shown in Fig. 4. The results for a two-dimensional 12% parabolic airfoil at M = 0.8 and an axisymmetrical body of revolution of a 10% parabolic arc profile at M = 0.975 are given in Figs. 5 and 6, respectively. For both two-dimensional and axisymmetrical cases, the agreement between the predicted effective shape and the reference calculation are very good. Now that effective shape has been determined, the next task is to determine the correction.

Global Mach Number Correction

The concept of global Mach number correction assumes that there exists an equivalent Mach number in free air where the calculated pressure distribution at a corrected Mach number will match the tunnel pressure distribution on the model or in a surface near the model as on the current procedure and simulation. This equivalent or corrected Mach number (M_C) is computed using the effective shape determined from the iterative procedure. Setting the free-air Mach number equal to the tunnel

Mach number ($M_f = M_t$), free-air calculations are performed exterior to the surface near the model. Comparisons of the pressure distribution for the axisymmetric case are shown in Fig. 7. Correcting the free-air Mach number from $M_f = 0.975$ to $M_c = 0.925$ resulted in a very good match between the free-air pressure distribution determined at M_c and the tunnel pressure distribution determined from the iterative procedure as shown in Fig. 7. Therefore, these tunnel data at $M = 0.975$ correspond to those in free air at $M = 0.925$.

Concluding Remarks

A method of the wall interference assessment/correction for transonic flow conditions has been developed using a two-component measured flow boundary condition approach successfully. The method avoids the difficulty of modeling the test article and the tunnel wall boundary conditions. The prediction of interferences includes subsonic and transonic flow regimes without the limitation on the selection of equations.

References

1. Lo, C. F., "Tunnel Interference Assessment by Boundary Measurements," AIAA Journal, April 1978.

2. Lo, C. F. and Sickles, W. L., "The Adaptive Wall Method for Two-Dimensional and Axisymmetrical Wind Tunnel," AEDC-TR-79-55, November 1979.

3. Kraft, E. M. and Dahm, W.J.F., "Direct Assessment Wall Interference in a Two-Dimensional Subsonic Wind Tunnel," AIAA Paper No. 82-0187, January 1982.

4. Mokry, M., Chan, Y. Y., and Jones, D. J., "Two-Dimensional Wind Tunnel Wall Interference," AGARDograph No. 281, November 1983.

5. Schairer, E. T., "Two-Dimensional Wind Tunnel Interference from Measurements on Two Contours," Journal of Aircraft, June 1984.

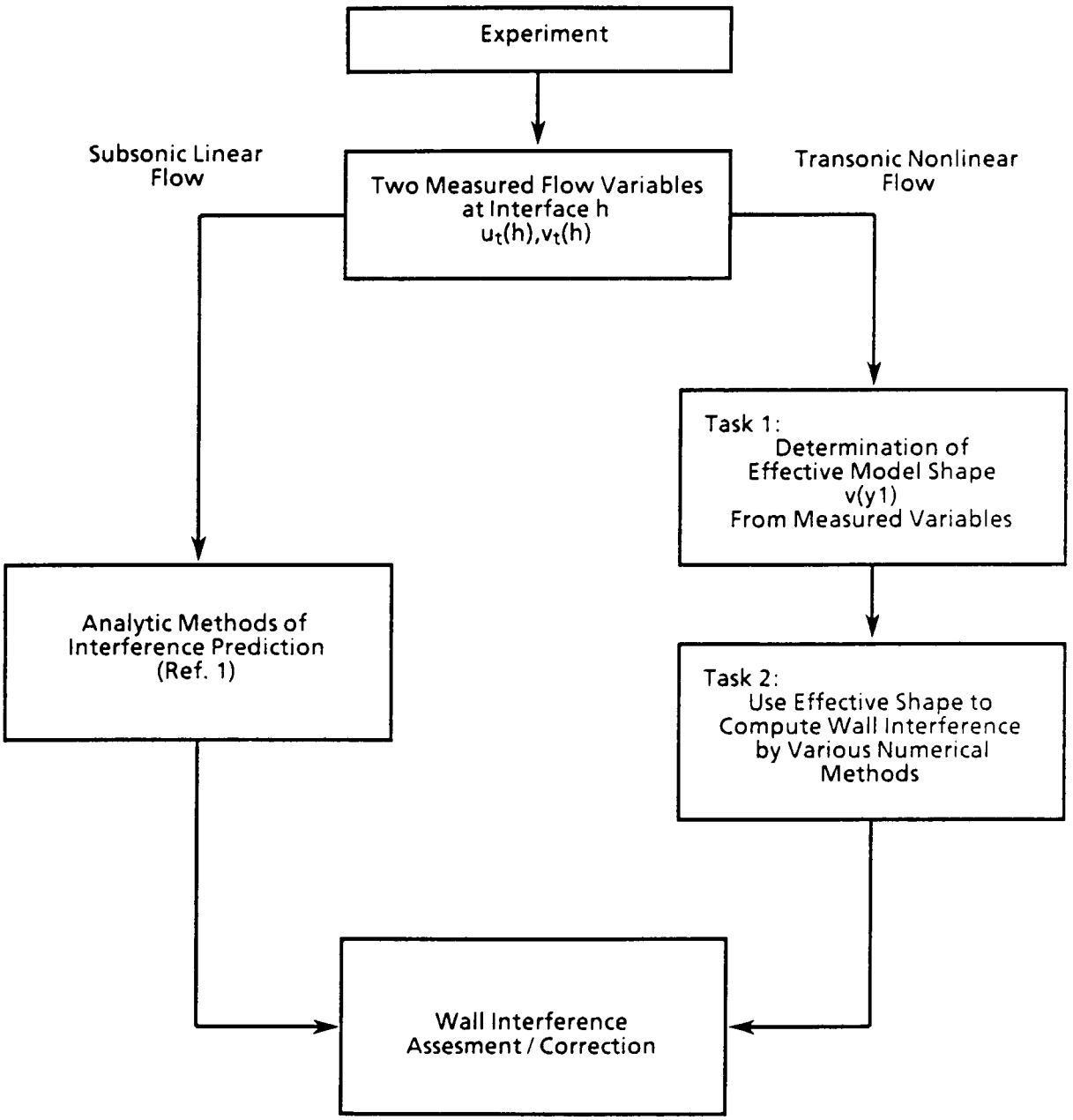

Figure 1. Prediction methods of wall interference assessment/correction using two measured variables at interface.

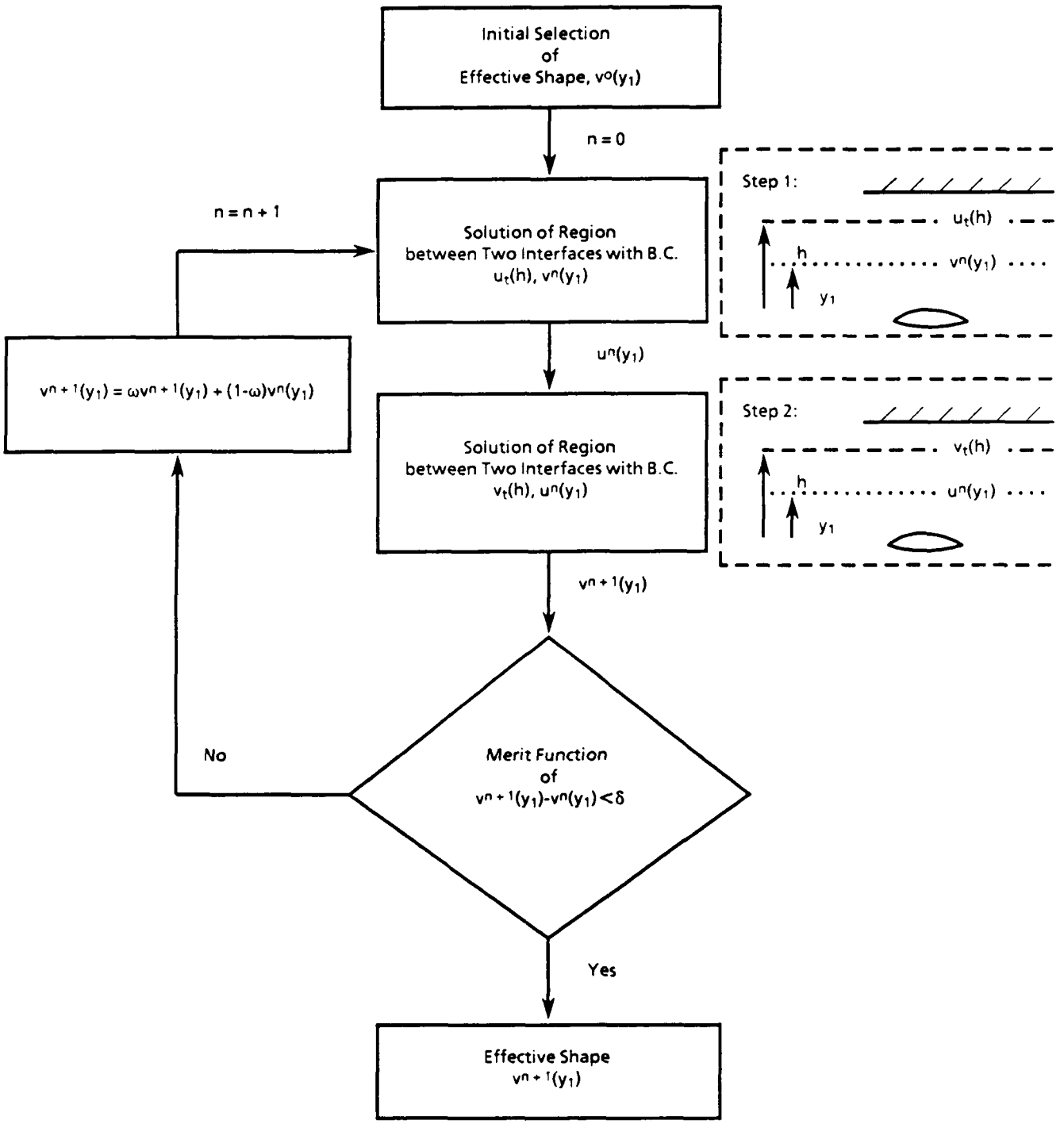

Figure 2. Iterative procedure for obtaining effective flow shape at $y = y_1$ by using measured variables, $u_t(h)$ and $v_t(h)$.

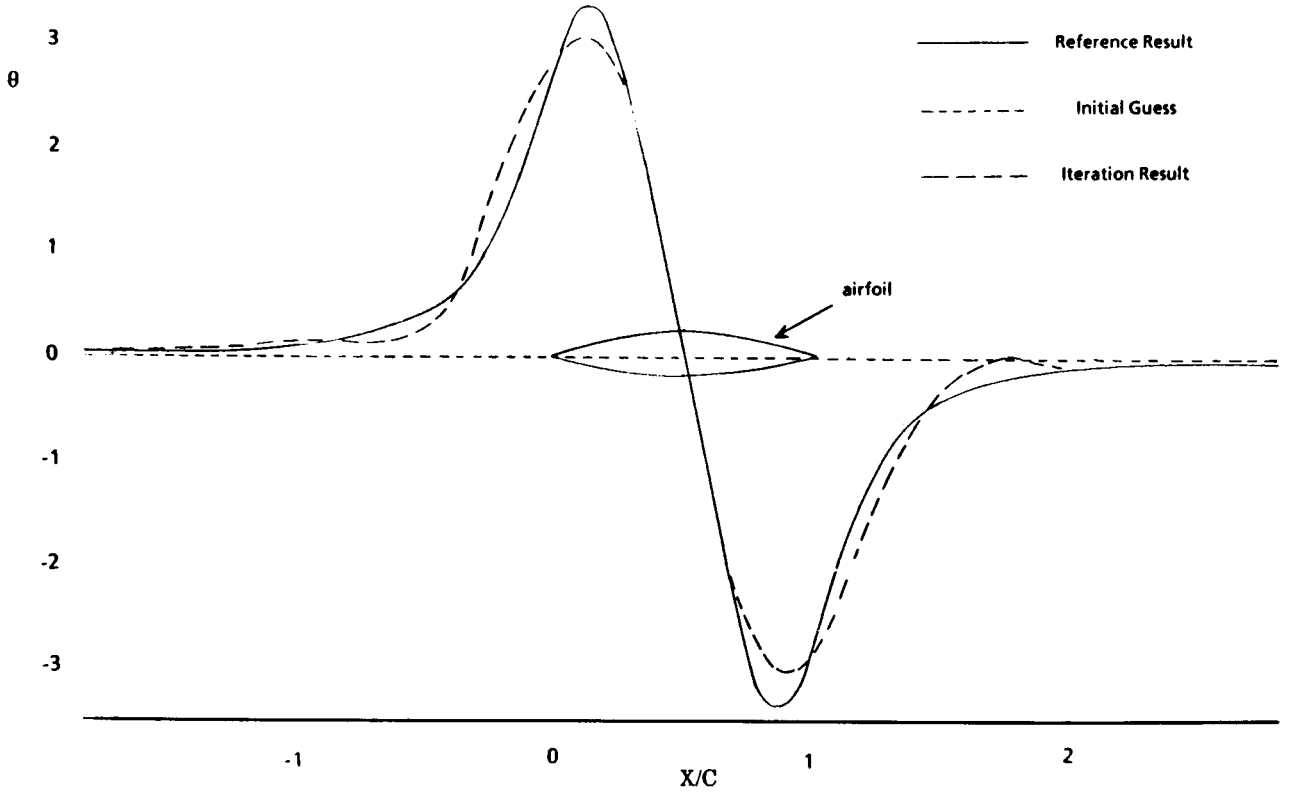

Figure 3. Comparison of results between iterative procedure with analytic expressions and reference calculation for NACA 0012, M = 0.6.

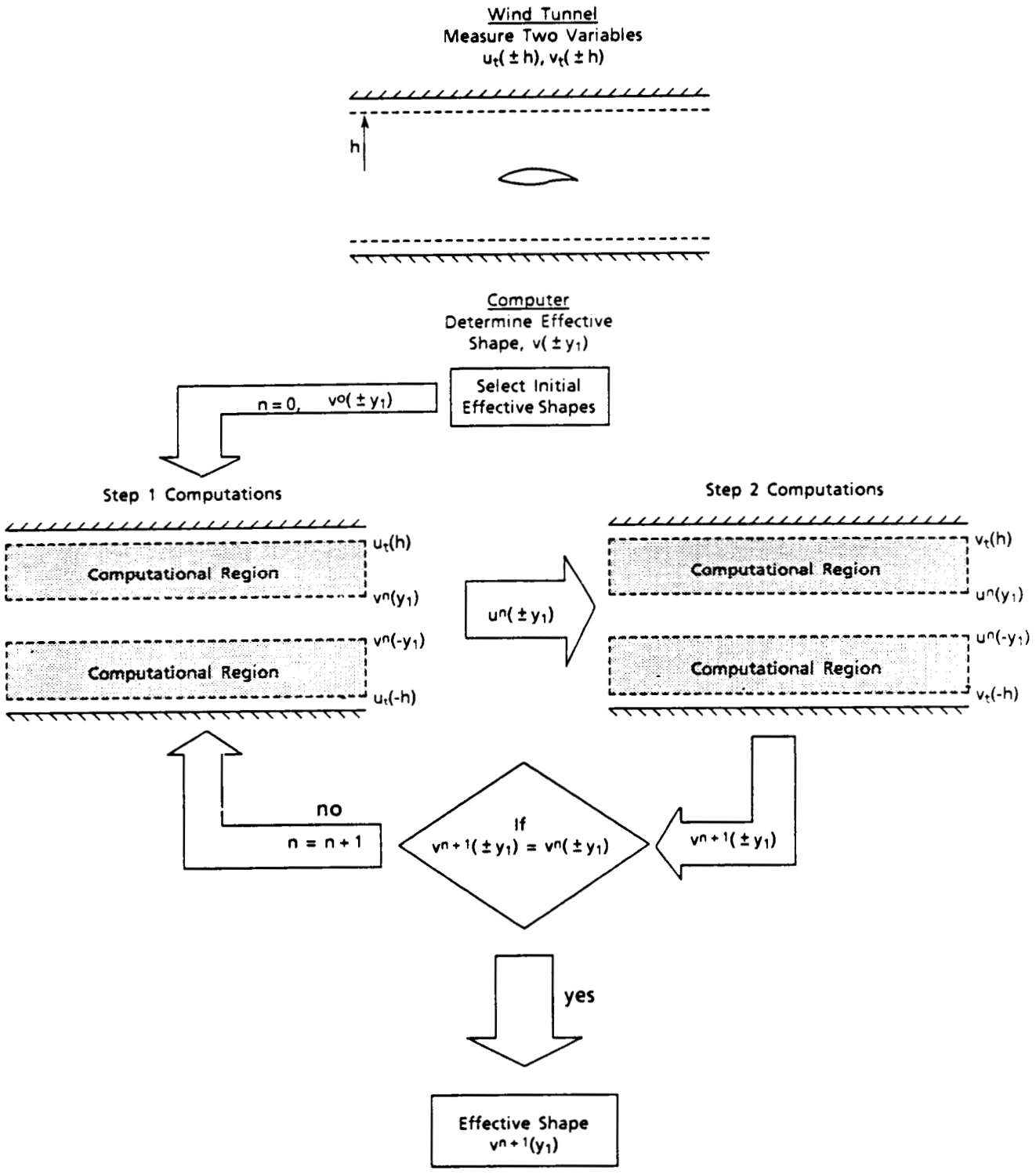

Figure 4. Two-variable numerical procedure to determine effective shape.

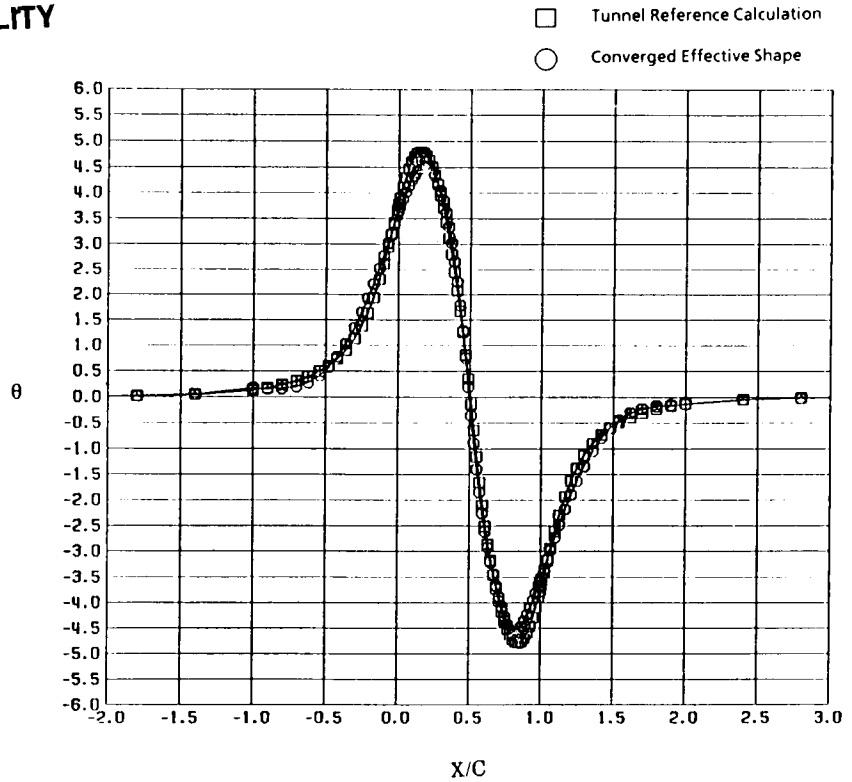

Figure 5. Predicted effective shape for two-dimensional case over 12% parabolic airfoil at $M_t = 0.8$, $\alpha = 0$, $y_1 = 0.3$, $h = 1$, $v^0 = (x,y_1) = 0$, open jet tunnel.

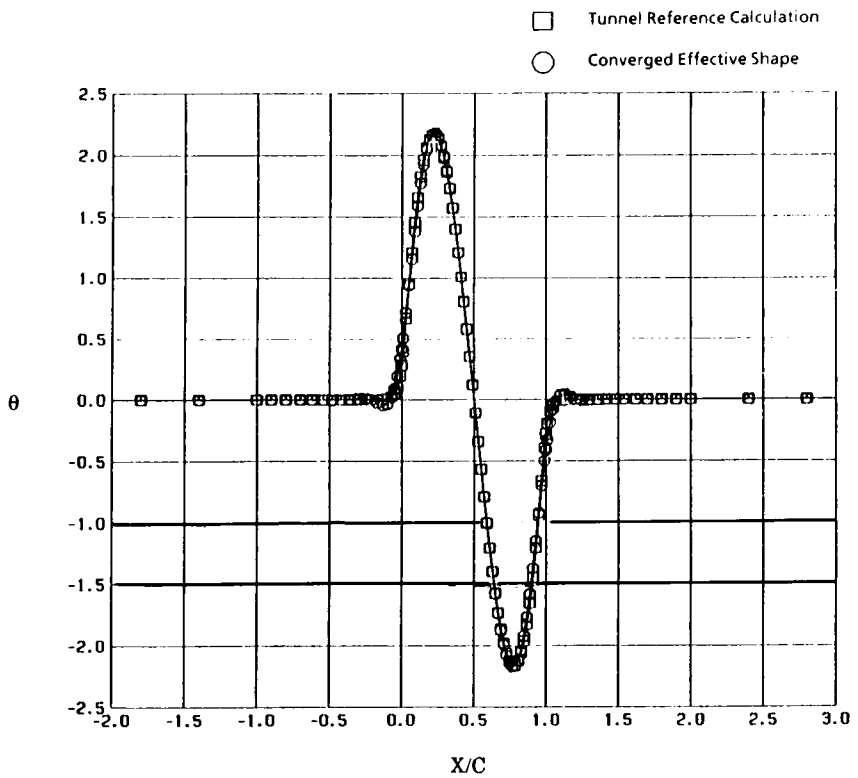

Figure 6. Predicted equivalent shape for axisymmetric case over 10% parabolic arc body at $M_t = 0.975$, $r_1 = 0.1$, $h = 0.5$, $v^0(x,r_1) = 0$, open jet tunnel.

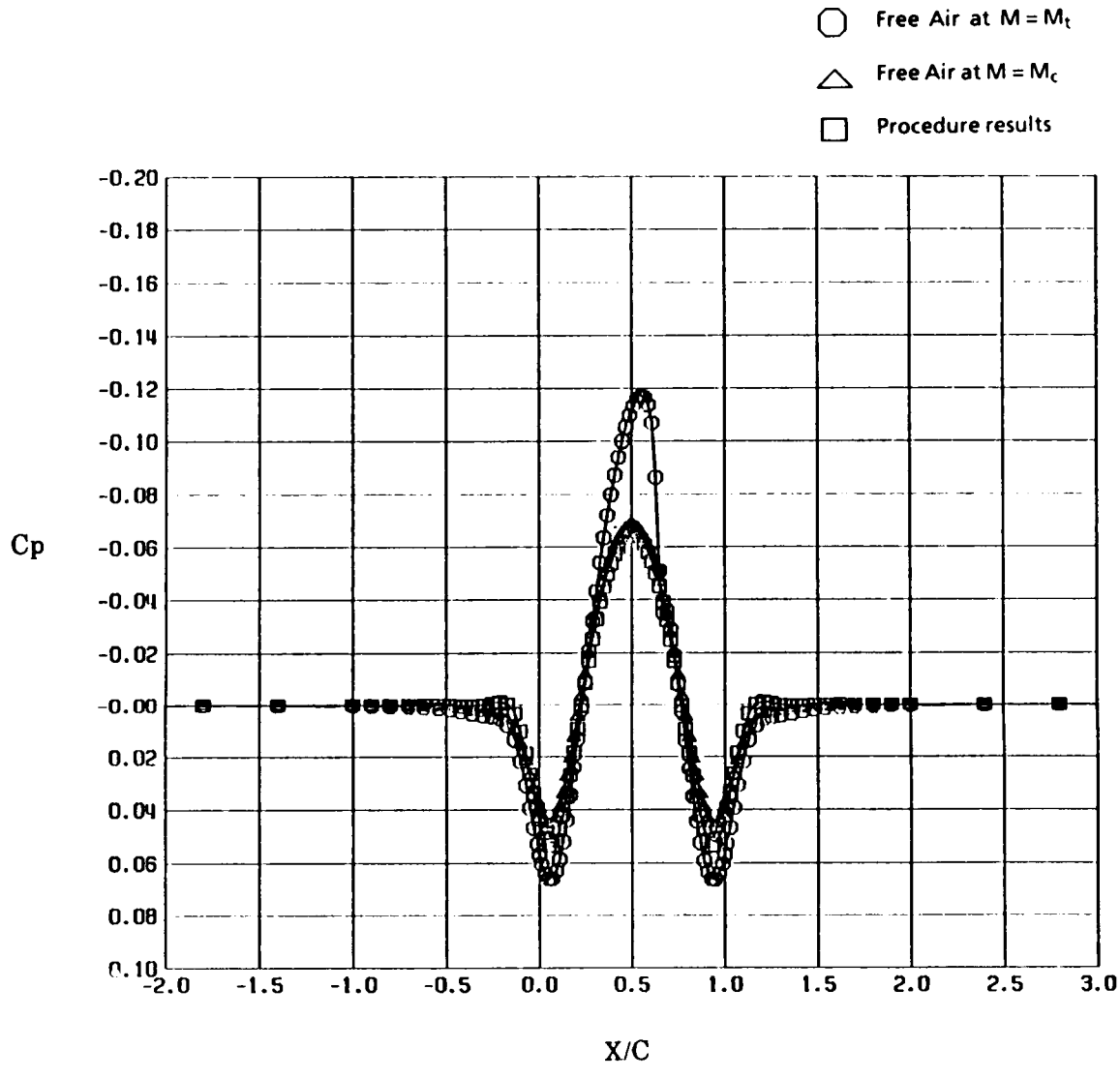

Figure 7. Pressure distributions for tunnel flow at M_t = 0.975 and free flight flow at M_c = 0.925.

Appendix A. Convergence of the Iterative Procedure

For the convenience of mathematical manipulation, the Fourier Transform technique is applied to prove the convergence of the iterative procedure. In the transform plane, the solution for $u(y_1)$ at $y = y_1$ for Step 1 in Eq. (1) is of the form

$$\bar{u}^{(n)}(p,y_1) = \frac{\bar{u}_t(p,h)}{\cosh p\beta(h-y_1)} - \frac{i}{\beta}\bar{v}^{(n)}(p,y_1)\tanh p\beta(h-y_1) \tag{A-1}$$

The boundary conditions applied to obtain the solution $u^{(n)}(y_1)$ are $u_t(h)$ measured and $v^{(n)}(y_1)$ selected. For Step 2, the solution for $v(y_1)$ of Eq. (2) can be expressed in the transform plane as

$$\bar{v}^{(n+1)}(p,y_1) = \frac{\bar{v}_t(p,h)}{\cosh p\beta(h-y_1)} - i\beta\,\bar{u}^{(n)}(p,y_1)\tanh p\beta(h-y_1) \tag{A-2}$$

where $u^{(n)}(y_1)$ is obtained from Eq. (A-1) of step 1 and $v_t(h_1)$ is measured.

Substituting $u^{(n)}(y_1)$ from Eq. (A-1) into Eq. (A-2), one obtains a single expression which can be used to start the iterative procedure as described in the previous section

$$\bar{v}^{(n+1)}(p,y_1) = \frac{\bar{v}_t(p,h)}{\cosh p\beta(h-y_1)} - i\beta\,\bar{u}_t(p,h)\frac{\sinh p\beta(h-y_1)}{\cosh^2 p\beta(h-y_1)} + \bar{v}^{(n)}(p,y_1)\tanh^2 p\beta(h-y_1) \tag{A-3}$$

This single expression, Eq. (A-3), can be utilized to prove the convergence of the iterative procedure. For simplicity the iterative expression, Eq. (A-3) is written in the following function form,

$$\bar{v}^{(n+1)} = G(\bar{u}_t, \bar{v}_t) + K\,\bar{v}^{(n)} \tag{A-3a}$$

where

$$G(u_t,v_t) = \frac{\bar{v}_t(p,h)}{\cosh p\beta(h-y_1)} - i\beta\,\bar{u}_t(p,h)\frac{\sinh p\beta(h-y_1)}{\cosh^2 p\beta(h-y_1)} \tag{A-3b}$$

and

$$K = \tanh^2 p\beta(h-y_1)$$

Before carrying successive substitution of each iteration, we can obtain the converged solution directily from Eq. (A-3a) as $v^{(n+1)} = v^{(n)} = v$

$$\bar{v} = G\frac{1}{1-K} \tag{A-4}$$

It should be noted that the solution of Eq. (A-4) in the physical plane is an integral equation of the first kind which is unstable and difficult to solve (see Appendix B). Thus, we choose Eq. (A-3) to obtain the present solution in an iterative fashion.

Let the initial guess be $V^{(o)}(y_1)$, the n-th iteration gives

$$\bar{v}^{(n)} = G + GK + GK^2 + \ldots + GK^{n-1} + \bar{v}^{(o)}K^n = G\,\frac{1-K^n}{1-K} + \bar{v}^{(o)}K^n \qquad \text{(A-5)}$$

Since $K = \tanh^2 p\beta\,(h-y1) < 1$,

$$\lim_{n\to\infty} \bar{v}^{(n)} = G\,\frac{1}{1-K}\,.$$

which converges to Eq. (A-4) as we wish to prove.

Appendix B. Stability of the Iterative Procedure

Before examining the stability of the iterative procedure, we investigate the explicit solution Eq. (A-4) in the physical plane. Equation (A-4) in the physical plane can be expressed as an integral equation of the first kind

$$\oint_{-\infty}^{\infty} = \frac{\bar{v}(\zeta)d\zeta}{\cosh\frac{\pi(\zeta-x)}{2\beta h}} = 2\beta h\, v_t(x,h) + \beta \oint_{-\infty}^{\infty} \frac{u_t(\zeta,h)d\zeta}{\sinh\frac{\pi(\zeta-x)}{2\beta h}} \tag{B-1}$$

The effects of measurement errors of u_t, v_t on the effective shape will be evaluated by the following assumed errors

$$v_{t_{err}}(x,h) = \frac{1}{a}\sin ax \tag{B-2}$$

where a is a parameter. The measurement error will vanish as a approaches infinity.

The result of effective shape due to $v_{t_{err}}$ of Eq. (B-2) obtained from Eq. (B-1) is

$$v_{err}(x) = \frac{1}{a}\sin ax \cdot \cosh a\beta h \tag{B-3}$$

As the $v_{t_{err}}$ decreases to the vanishing small as $a \to \infty$, the error of effective shape is magnified to an arbitrarily large value

$$Max\left|v_{err}(x)\right| = \left|\frac{1}{a}\cosh a\beta h\right| \to \infty \ as\ a \to \infty \tag{B-4}$$

This demonstrates that the formulation of Eq. (B-1) is not stable, since a small measurement error in the boundary flow quantities will result in the effective shape of Eq. (B-4) growing to an arbitrarily large amount. On the other hand, we will demonstrate that the iterative procedure is stable as follows.

We assume that the measurement error of v_t and u_t of the forms

$$v_{t_{err}}(x,h) = \frac{1}{a}\cos ax \tag{B-5}$$

$$u_{t_{err}}(x,h) = \frac{1}{a}\cos ax$$

The error of the effective shape obtained from Eqs. (1) and (2) is:

$$v_{t_{err}}(x) = \frac{\cos ax}{a}\frac{1}{\cosh a\beta h} - \beta\frac{\sin ax}{a}\frac{\tanh a\beta h}{\cosh a\beta h} \tag{B-6}$$

when the measured error vanishes as $a \to \infty$, the error of effective shape Eq. (B-6) will also vanish. This indicates that the iterative procedure is stable as the measured input is perturbed.